THE JOURNAL OF BIOLOGICAL CHEMISTRY VOL. 286, NO. 24, pp. 21511–21523, June 17, 2011

A Novel GDP-D-glucose Phosphorylase Involved in Quality Control of the Nucleoside Diphosphate Sugar Pool in *Caenorhabditis elegans* and Mammals*[S]

Received for publication, March 9, 2011, and in revised form, April 15, 2011 Published, JBC Papers in Press, April 20, 2011, DOI 10.1074/jbc.M111.238774

Lital N. Adler[‡1], **Tara A. Gomez**[‡], **Steven G. Clarke**[‡2], **and Carole L. Linster**[‡§3]

From the [‡]*Department of Chemistry and Biochemistry and the Molecular Biology Institute, UCLA, Los Angeles, California 90095 and the* [§]*de Duve Institute, Université Catholique de Louvain, 1200 Brussels, Belgium*

The plant *VTC2* gene encodes GDP-L-galactose phosphorylase, a rate-limiting enzyme in plant vitamin C biosynthesis. Genes encoding apparent orthologs of VTC2 exist in both mammals, which produce vitamin C by a distinct metabolic pathway, and in the nematode worm *Caenorhabditis elegans* where vitamin C biosynthesis has not been demonstrated. We have now expressed cDNAs of the human and worm *VTC2* homolog genes (*C15orf58* and *C10F3.4*, respectively) and found that the purified proteins also display GDP-hexose phosphorylase activity. However, as opposed to the plant enzyme, the major reaction catalyzed by these enzymes is the phosphorolysis of GDP-D-glucose to GDP and D-glucose 1-phosphate. We detected activities with similar substrate specificity in worm and mouse tissue extracts. The highest expression of GDP-D-glucose phosphorylase was found in the nervous and male reproductive systems. A *C. elegans C10F3.4* deletion strain was found to totally lack GDP-D-glucose phosphorylase activity; this activity was also found to be decreased in human HEK293T cells transfected with siRNAs against the human *C15orf58* gene. These observations confirm the identification of the worm *C10F3.4* and the human *C15orf58* gene expression products as the GDP-D-glucose phosphorylases of these organisms. Significantly, we found an accumulation of GDP-D-glucose in the *C10F3.4* mutant worms, suggesting that the GDP-D-glucose phosphorylase may function to remove GDP-D-glucose formed by GDP-D-mannose pyrophosphorylase, an enzyme that has previously been shown to lack specificity for its physiological D-mannose 1-phosphate substrate. We propose that such removal may prevent the misincorporation of glucosyl residues for mannosyl residues into the glycoconjugates of worms and mammals.

The last missing enzyme of the plant vitamin C biosynthesis pathway was recently identified as a GDP-L-galactose phosphorylase encoded by the *Arabidopsis VTC2* gene (1, 2). In this 10-step metabolic pathway from D-glucose to L-ascorbate, GDP-L-Gal[4] phosphorylase catalyzes the formation of L-Gal-1-P in the first committed (and highly regulated) step to vitamin C biosynthesis (2–5). Intriguingly, the *VTC2* gene appears to be conserved in vertebrates, which are known to synthesize vitamin C via a different metabolic pathway than plants that does not include GDP-L-Gal as an intermediate (6), and in invertebrates such as *Caenorhabditis elegans* that may lack the ability to synthesize vitamin C (1). The physiological functions of these apparent orthologs are thus unclear. One clue may be that the *Arabidopsis* VTC2 enzyme can also use GDP-D-glucose as a substrate (1). Although the role of this activity in plants is unclear, such an activity may be important in other species. Whereas GDP-L-Gal is most probably absent from mammalian tissues, the presence of GDP-D-Glc in bovine mammary gland and the existence of a mammalian GDP-D-Glc pyrophosphorylase have been reported (7, 8). More recent observations suggest that GDP-D-Glc formation can be catalyzed by the mammalian GDP-D-mannose pyrophosphorylase (9, 10). No metabolic role of GDP-D-Glc in mammalian tissues has been proposed, however, and nothing is known about this metabolite in *C. elegans*.

The *Arabidopsis* VTC2 protein and its invertebrate and vertebrate homologs are members of the histidine triad (HIT) superfamily of proteins, which includes nucleotide hydrolases and transferases (11). Known substrates of this superfamily of enzymes include AMP-lysine, diadenosine polyphosphate, AMP-sulfate, and nucleotide sugars such as UDP-D-Glc and ADP-D-Glc in addition to GDP-L-Gal (12). HIT enzymes are characterized by the presence of a H*X*H*X*(H/Q) motif (*X* represents a hydrophobic amino acid), the second histidine residue of which generally attacks the α-phosphate of the nucleotide substrate. This leads to release of the leaving group and nucleotidylation of the enzyme. The nucleotidylated enzyme is then resolved by either hydrolysis or, in the case of transferases and

* This work was supported, in whole or in part, by National Institutes of Health Grants GM026020 and AG032303 (to S. G. C.). This work was also supported by a Senior Scholar in Aging Award from the Ellison Medical Foundation (to S. G. C.).

[S] The on-line version of this article (available at http://www.jbc.org) contains supplemental Figs. S1–S3 and Tables S1 and S2.

[1] Supported by a UCLA Philip Whitcome Fellowship.

[2] To whom correspondence may be addressed: Dept. of Chemistry and Biochemistry and the Molecular Biology Inst., UCLA, 607 Charles E. Young Dr. E., Los Angeles, CA 90095. Tel.: 310-825-8754; Fax: 310-825-1968; E-mail: clarke@mbi.ucla.edu.

[3] Supported by the Fonds de la Recherche Scientifique (FNRS) and by the European Union Seventh Framework Programme (FP7/2007-2013) under grant agreement 276814. To whom correspondence may be addressed: de Duve Inst., Université catholique de Louvain, BCHM 7539, Ave. Hippocrate 75, B-1200 Brussels, Belgium. Tel.: 32-2-7647561; Fax: 32-2-7647598; E-mail: carole.linster@uclouvain.be.

[4] The abbreviations used are: GDP-L-Gal, GDP-β-L-galactose; ADP-D-Glc, ADP-α-D-glucose; D-Gal-1-P, α-D-galactose 1-phosphate; L-Gal-1-P, β-L-galactose 1-phosphate; GDP-D-Glc, GDP-α-D-glucose; GDP-D-Man, GDP-α-D-mannose; GDP-L-Fuc, GDP-β-L-fucose; D-Glc-1-P, α-D-glucose 1-phosphate; HIT, histidine triad; IP-LC-ESI-MS, ion pair liquid chromatography-electrospray ionization mass spectrometry; D-Man-1-P, α-D-mannose 1-phosphate; NDP, nucleoside diphosphate; UDP-D-Gal, UDP-α-D-galactose; UDP-D-Glc, UDP-α-D-glucose; LLO, lipid-linked oligosaccharide; CDG-I, congenital disorders of glycosylation type I.

phosphorylases, transfer to a second phosphorylated substrate or inorganic phosphate, respectively (4, 12).

In the present work, we overexpressed and purified the *C. elegans* and human *VTC2* homolog gene products (C10F3.4 and C15orf58, respectively) and determined their kinetic properties as well as their substrate specificities. We found that both genes encode GDP-D-Glc phosphorylases with properties very similar to each other and to GDP-D-Glc phosphorylase activity detected in *C. elegans* and mouse tissue extracts. We confirmed the molecular identity of this enzyme by using a *C10F3.4* worm deletion strain and by performing siRNA experiments in HEK293T cells. Based on the accumulation of GDP-D-Glc in *C. elegans* worms lacking the VTC2 homolog, we propose a physiological role for GDP-D-Glc phosphorylase in removing the GDP-D-Glc formed by the nonspecific enzyme GDP-D-mannose pyrophosphorylase to limit its misincorporation into glycoproteins and other glycoconjugates.

EXPERIMENTAL PROCEDURES

Materials—ADP-D-Glc, GDP-D-Glc, GDP-D-Man, UDP-D-Gal, UDP-D-Glc, D-Gal-1-P, D-Glc-1-P, D-Man-1-P (all of these nucleotide sugars and hexose phosphates were in the α-configuration), GDP-β-L-Fuc, GDP, glucose-6-P dehydrogenase from *Leuconostoc mesenteroides*, and β-nicotinamide adenine dinucleotide (NAD) were from Sigma. L-Gal-1-P was from Glycoteam (Hamburg, Germany). Phosphoglucomutase (α-D-glucose-1,6-bisphosphate:α-D-glucose-1-phosphate phosphotransferase) from rabbit muscle was purchased from OYC Americas (Andover, MA). All other reagents were of analytical grade. GDP-β-L-Gal, synthesized and purified as described (13), was provided by Prof. Shinichi Kitamura (Osaka Prefecture University). This preparation was further purified by the reverse-phase HPLC method described previously (1). Fractions containing GDP-L-Gal were lyophilized, resuspended in H_2O, and stored at −20 °C.

C. elegans Strains and Culture Conditions—Standard procedures used to maintain *C. elegans* strains were adapted from Sulston and Hodgkin (14). M9 and S media were prepared as described by Lewis and Fleming (15). The N2 strain was obtained from the *Caenorhabditis* Genetics Center (St. Paul, MN). The *C10F3.4* mutant strain (*tm2679*) lacking coding sequences between exons 5 and 8 of the *C10F3.4* gene (WormBase), was provided by the *C. elegans* Core Facility at Tokyo Women's Medical University. We also used a transgenic strain expressing a C10F3.4::GFP fusion protein under the endogenous *C10F3.4* promoter (see "Transgenic Worm Construction and Analysis"). *C. elegans* strains were cultured at 20 °C according to standard procedures (16). All strains were maintained at 20 °C on nematode growth medium plates streaked with *Escherichia coli* OP50 (14). Liquid cultures of these worm strains were grown at 20 °C in S medium supplemented with concentrated *E. coli* OP50, and worms were harvested, washed, and sucrose-floated as described previously (17) except that M9 medium was used instead of 0.1 M NaCl as a resuspension and washing solution.

Transgenic Worm Construction and Analysis—The C10F3.4::GFP fusion construct and the transgenic lines expressing the C10F3.4::GFP fusion protein were generated at the Worm Core Facility (University of Utah). The C10F3.4::GFP construct, placing the *C10F3.4* gene as well as the 3-kb genomic region immediately upstream of the *C10F3.4* transcription start site in-frame with GFP, was made via a PCR fusion procedure described previously (18). The primer sequences used for this fusion procedure were as follows: 5′-TGATCAGTTGGGACCCACCATGAG-3′, 5′-CTTTGGCCAATCCCGGGGATCTTTCGATCCCTCGTCAGATTGAGC-3′, 5′-GCTCAATCTGACGAGGGATCGAAAGATCCCCGGGATTGGCCAAAG-3′, and 5′-AGCACGAACAACTCGGGGTGA-3′. The C10F3.4::GFP fusion construct was injected at 5 ng/μl along with 80 ng/μl pRF4 and pBlueScript KS at 35 ng/μl into the gonad arms of N2 adult hermaphrodites. Transgenic animals of the N2 *xtEX85(C10F3.4::GFP, pRF4)* genotype were identified by the Rol phenotype, and stable lines were isolated. The isolated line used in this study was designated *UZ119*.

Cloning and Expression of C. elegans C10F3.4—The *C. elegans C10F3.4a* coding sequence was PCR-amplified from an Invitrogen ProQuest *C. elegans* cDNA library in the vector pPC86 (catalog number 11288-016) using forward primer 5′-CACCATGGAGCCTTTTCCGCGAATC-3′ and reverse primer 5′-TCATTTCGATCCCTCGTCAGATTG-3′. The ProQuest cDNA library was prepared from RNA extracted from a mixed population of adult and larval nematode worms of the N2 strain. The PCR product was purified and cloned into the Champion pET100/D-Topo vector (Invitrogen), and the recombinant plasmid was transformed into *E. coli* BL21 Star (DE3) cells. The transformed *E. coli* cells were grown at 37 °C in LB medium containing 50 μg/ml carbenicillin (Sigma) until the optical density at 600 nm reached a value of about 0.6. Recombinant protein production was induced by the addition of 0.4 mM isopropyl β-D-thiogalactopyranoside. After overnight incubation with shaking at 18 °C, cells were harvested, washed, and frozen at −80 °C. Cells were then thawed; resuspended in a pH 8.0 buffer containing 50 mM sodium phosphate, 500 mM NaCl, 5 mM β-mercaptoethanol, 5% glycerol, Roche Applied Science Complete protease inhibitor mixture (1 tablet/50 ml), and 10 units/ml Benzonase nuclease (Novagen); and lysed by sonication as described (19). The lysate was centrifuged for 60 min at 13,000 × *g* at 4 °C. The resulting supernatant was loaded onto a 5-ml HisTrap HP nickel affinity column (GE Healthcare), and His-tagged C10F3.4 protein was eluted using a gradient of 20–500 mM imidazole according to the manufacturer's specifications. Peak protein fractions containing the C10F3.4 protein were pooled, and buffer was exchanged to 10 mM HEPES, pH 7.5, 100 mM NaCl, and 1 mM dithiothreitol in a 10-kDa-cutoff Amicon Ultra centrifugal filter unit (Millipore, Billerica, MA). Protein concentration was determined using a Lowry assay after precipitation with 10% trichloroacetic acid. SDS-PAGE analysis of the purified enzyme preparation used throughout this study revealed a single band at the expected molecular weight for the His-tagged C10F3.4 protein after Coomassie Blue staining. The purified enzyme was stored at −80 °C in 10% glycerol.

Cloning and Expression of Human C15orf58—The Human ORFeome Collaboration Clone 100016258, a Gateway Entry vector containing the predicted complete cDNA coding sequence of the human *C15orf58* gene (GenBank™ accession number BC153017), was purchased from Open Biosystems

(Huntsville, AL). This Entry clone was used in LR recombination reactions (Invitrogen) with the T7 promoter expression vector pDEST17 to obtain a construct for production of recombinant C15orf58 protein with an N-terminally fused hexahistidine tag as described by the manufacturer. This construct was transformed into *E. coli* BL21 Star (DE3) cells for protein overexpression. Recombinant human C15orf58 protein was produced and purified as described for recombinant *C. elegans* C10F3.4 protein with the exception that a 5–500 mM imidazole gradient was used for elution of His-tagged C15orf58. Protein concentration was determined using a Lowry assay after precipitation with 10% trichloroacetic acid. Protein purity was determined by SDS-PAGE analysis using Coomassie Blue staining followed by densitometry using the NIH ImageJ software; recombinant C15orf58 protein was estimated to represent 17% of the total protein present in the enzyme preparation used throughout this study. The contaminating proteins present in this preparation did not interfere with our enzymatic assays (absence of significant hydrolytic activities acting on GDP-sugars or GDP), and recombinant C15orf58 was therefore not purified further. The purified enzyme preparation was stored at −80 °C in 10% glycerol.

siRNA Transfection and Extraction of HEK293T Cells—HEK293T cells were maintained in Dulbecco's modified Eagle's medium (DMEM) supplemented with 10% heat-inactivated fetal calf serum, 1% penicillin/streptomycin, and 2 mM Ultra-Glutamine in an atmosphere of 5% CO_2 in air. For transfection of cells with siRNAs, HEK293T cells were plated at a density of about 800,000 cells/9.6-cm^2 well. Cells were transfected the following day using 50 nM control siRNA (Dharmacon ON-TARGETplus non-targeting pool from Thermo Scientific (Epsom, UK)) or 50 nM *C15orf58* siRNA (Dharmacon ON-TARGETplus SMARTpool from Thermo Scientific) and 6 μl of the transfection reagent Lipofectamine 2000 (Invitrogen) in the absence of antibiotics in the culture medium according to the manufacturer's instructions. The culture medium was replaced by fresh medium containing antibiotics about 6 h after addition of the RNA-Lipofectamine 2000 complexes. After 48–72 h, the cells were either washed with cold phosphate-buffered saline (PBS) and resuspended in lysis buffer containing 25 mM HEPES, pH 7.1, 5 μg/ml antipain, and 5 μg/ml leupeptin for protein extraction or resuspended in TriPure Isolation Reagent (Roche Applied Science) for total RNA extraction. For protein extraction, cells were lysed by one cycle of freeze-thawing and centrifuged. The resulting supernatant was used to assay GDP-D-Glc phosphorylase activity by the HPLC method described below. Protein concentration in these extracts was determined by the Lowry assay after protein precipitation with 10% trichloroacetic acid. Total RNA was isolated from the TriPure cell extracts after phase separation using chloroform according to the manufacturer's instructions. The RNA concentration was determined by measuring the absorbance at 260 nm, and the samples were stored at −80 °C.

Quantitative Real Time PCR—To measure *C15orf58* transcript levels in siRNA-transfected HEK293T cells, cDNA was synthesized using RevertAid™ H Minus reverse transcriptase (Fermentas, St. Leon-Rot, Germany) and random hexamers according to the manufacturer's protocol and adding 1 μg of RNA in a total volume of 20 μl. We used 5 μl of 20-fold diluted reverse transcription reaction in subsequent 25-μl quantitative real time PCR reactions run in a MyiQ™ thermal cycler with SYBR Green as a fluorescent dye (Bio-Rad), HotStart *Taq* polymerase (Eurogentec, Seraing, Belgium), and 0.3 μM gene-specific forward and reverse primers. PCR programs were 95 °C for 5 min, 40 cycles at 95 °C for 10 s, and 60 °C for 1 min with acquisition of fluorescence information followed by a melting curve. Experiments shown represent averages for four biological replicates. Primers used for amplification can be obtained upon request.

Protein and Small Molecule Extraction from C. elegans and Mouse Tissues—All steps of the described extraction procedures were carried out at 4 °C. Brain, heart, liver, kidney, thymus, and testes of C57BL6 mice were removed as quickly as possible from sacrificed animals; frozen in liquid nitrogen; and stored at −80 °C until further extraction. For protein extraction, the frozen tissues were placed in 3 volumes (v/w) of lysis buffer (50 mM Tris-HCl, pH 7.5, 1 mM dithiothreitol, 2 mM EDTA, 10% glycerol, Roche Complete protease inhibitor mixture (1 tablet/50 ml), and 1 mM phenylmethylsulfonyl fluoride) and homogenized in a Potter-Elvehjem apparatus. The homogenates were centrifuged at 21,000 × *g* for 40 min, and the supernatants were stored for enzymatic assays. For small molecule extraction, the frozen tissues were homogenized in a Potter-Elvehjem apparatus after addition of 2 volumes (v/w) of 10% perchloric acid. After centrifugation of the homogenates at 21,000 × *g* for 40 min, the supernatants were neutralized with K_2CO_3.

Worms, harvested as described above, were resuspended in 2 volumes (v/w) of lysis buffer or 1 volume (v/w) of 10% perchloric acid. The worm suspensions were freeze-dropped in liquid nitrogen and ground to a fine powder in a precooled mortar and pestle. The homogenates were allowed to thaw on ice and centrifuged at 21,000 × *g* for 30 min. The supernatants of the perchloric acid extracts were neutralized with K_2CO_3. All protein and small molecule extracts were stored at −80 °C until assayed for enzymatic activity or GDP-hexose content. Protein concentration was determined using the Lowry assay after protein precipitation with 10% trichloroacetic acid.

HPLC-based Nucleoside Diphosphate (NDP)-hexose Phosphorylase Assay—NDP-hexose phosphorylase activities of recombinant enzymes, worm and mouse tissue extracts, and HEK293T cell extracts were assayed by measuring NDP formation after incubation with NDP-hexose in a reaction mixture at pH 7.5 containing 50 mM Tris-HCl or HEPES, 5 mM sodium phosphate, 0 or 2 mM $MgCl_2$, 0 or 1 mM EDTA, 10 mM NaCl, and 1 mM dithiothreitol. Recombinant enzymes, worm extracts, and HEK293T cell extracts were generally assayed without $MgCl_2$ and always without EDTA in the reaction mixture. Mouse tissue extracts were assayed in the absence of $MgCl_2$ and in the presence of 1 mM EDTA. The salt and small molecule content of worm, mouse tissue, and HEK293T cell extracts was minimized by processing them on spin desalting columns (Thermo Scientific, Rockford, IL) immediately before using them for activity measurements. Desalting, omission of externally added Mg^{2+}, and/or addition of EDTA allowed minimization of NDP-hexose hydrolysis by contaminating nucleotide

pyrophosphatase activities. Additionally, desalting of the protein extracts allowed the removal of compounds prone to interfere with the enzymatic assay (inorganic phosphate, nucleotides, and nucleotide derivatives). Reactions (at 26 °C for *C. elegans* enzyme preparations and at 31 °C for mammalian enzyme preparations) were initiated by enzyme addition and stopped after 5–30 min by heating at 98 °C for 3 min. After removal of precipitated protein by centrifugation, supernatants were analyzed by anion exchange HPLC as described (1). NDP and NDP-hexose concentrations were calculated by comparing the integrated peak areas with those of standard NDP or NDP-hexose solutions.

Spectrophotometric GDP-D-Glc Phosphorylase Assay—The GDP-D-Glc phosphorylase activity of worm and human recombinant enzymes was also measured by a spectrophotometric assay modified from Nihira *et al.* (20). Briefly, a reaction mixture containing 60 mM Tris-HCl, pH 7.5, 2.4 mM NAD, 0–20 mM sodium phosphate, 12 mM $MgCl_2$, 12 mM NaCl, 1.2 mM dithiothreitol, 0–100 μM GDP-D-Glc, 6 IU/ml phosphoglucomutase, and 6 IU/ml glucose-6-P dehydrogenase was prepared, and 250 μl of this mixture were added per well in a 96-well plate. The latter was transferred to a plate reader (Molecular Devices, Sunnyvale, CA) that monitored the absorbance at 340 nm. Recombinant enzyme was added after an ~5-min preincubation at 26 or 31 °C, and linear production of NADH was measured by ΔA_{340} over a 10-min time period to determine the rate of conversion of GDP-D-Glc to D-Glc-1-P. The light path length for each well was measured via the plate reader SoftMax Pro5 software before addition of the enzyme.

Microscopy—Nematodes were anesthetized using levamisole (2 mg/ml) and mounted on 2% agarose pads. Cells were identified by comparing the position of GFP-positive areas viewed by simultaneous fluorescence and differential interference contrast microscopy. Images were captured using a Zeiss Axioscope (Thornwood, NY) at 40× power magnification with an attached Hamamatsu Orca-ER camera (Bridgewater, NJ) and Volocity software (Improvision, Lexington, MA). All images shown in this study were prepared by using Adobe Photoshop Elements 8.0 software (San Jose, CA).

GDP-D-hexose Detection and Assay by Ion Pair Liquid Chromatography-Electrospray Ionization Mass Spectrometry (IP-LC-ESI-MS)—All experiments were carried out on an Agilent 1200 HPLC system coupled to a 4000 QTRAP MS/MS hybrid triple quadrupole/linear ion trap mass spectrometer from Applied Biosystems (Foster City, CA). The HPLC system was equipped with a PAL autosampler with thermostated tray holders and stack (LEAP Technologies, Carrboro, NC). The turbo electrospray ionization source of the 4000 QTRAP system was operated in the negative ion mode. Q1 and Q3 were operated in unit resolution. All system control, data acquisition, and mass spectral data evaluation were performed using Analyst software version 1.4.2 from Applied Biosystems. The GDP-D-hexose assay was based on the procedure of Coulier *et al.* (21). A Luna 3-μm C_{18}(2) column (150 × 3.0 mm, Phenomenex) was used with a Luna C_{18} security guard cartridge (4 × 3.0 mm, Phenomenex). Mobile phase A consisted of 10 mM hexylamine as an ion pairing agent (Aldrich) in water adjusted to pH 6.3 with acetic acid. Mobile phase B consisted of 90% methanol, 10% 10 mM ammonium acetate, and 7.5 mM hexylamine adjusted to pH 8.9 with ammonium hydroxide. A mobile phase gradient was used with a flow rate of 0.4 ml/min starting at 100% A for 15 min followed by a linear gradient from 100 to 65% A over 18 min, then holding at 65% A for 2 min followed by a linear gradient from 65 to 100% A in 2 min, and finally holding for 13 min at 100% A. The column temperature was maintained at 40 °C, and the injection volume was 10 μl. Mass detection was carried out in the negative mode under the following conditions: spray voltage at −4.5 kV, heated capillary temperature at 550 °C, curtain gas at 25, and collision gas at the medium setting. The system was tuned using a stock solution of GDP-D-Glc or GDP-D-Man (10 μM) in water. The precursor-to-product ion transitions in multiple reaction monitoring mode used to detect GDP-D-Glc and GDP-D-Man were as follows: m/z 604 → 362, m/z 604 → 158, m/z 604 → 210, and m/z 604 → 343. Both GDP-hexoses yielded the same precursor ion, m/z 604, which produced the same four product ions (m/z 158, 210, 343, and 362). However, the relative abundances at which these product ions were generated differed between the two GDP-hexoses, and we chose product ion m/z 604 → 362 to detect and quantify GDP-D-Glc, whereas product ion m/z 604 → 158 was used to detect and quantify GDP-D-Man.

RESULTS

Characterization of C. elegans and Human Homologs of Arabidopsis VTC2—The *Arabidopsis VTC2* gene has recently been shown to encode GDP-L-Gal phosphorylase, a highly regulated enzyme that catalyzes the first committed step in the plant vitamin C synthesis pathway (4). The presence of VTC2 homologs in species that synthesize vitamin C via a metabolic pathway different from that of plants (most non-primate mammals), in species that do not synthesize vitamin C (*e.g.* primates including humans), or in species where vitamin C synthesis has not been generally established (invertebrates) (6, 22, 23) stimulated us to characterize the human and *C. elegans* proteins to understand their physiological function. These proteins share 25–30% sequence identity over their enzyme length with VTC2 from *Arabidopsis thaliana* (1). cDNAs of the human *VTC2* homolog gene (*C15orf58*) and the *C. elegans VTC2* homolog gene (*C10F3.4*) were overexpressed in a bacterial expression system as N-terminally His-tagged proteins and affinity-purified on Ni^{2+} columns.

Interestingly, the Gln residue of the conserved H*X*H*X*Q motif in the plant VTC2 protein is replaced by a His residue in the mammalian and invertebrate homolog proteins including human C15orf58 and worm C10F3.4. The resulting H*X*H*X*H motif constitutes the histidine triad motif generally found in the nucleotide hydrolase branch of the HIT protein superfamily, whereas H*X*H*X*Q is the signature motif of the nucleotide transferase branch of this protein superfamily (12). To find out whether the human and worm proteins act as nucleotide hydrolases or transferases, we tested the activity of the recombinant enzymes on GDP-D-Glc, the preferred substrate for plant VTC2 after GDP-L-Gal, in the absence or presence of various potential nucleotide acceptors including inorganic phosphate (P_i), inorganic pyrophosphate (PP_i), L-Gal-1-P, and D-Man-1-P (supplemental Fig. S1). The enzymatic activities

TABLE 1

Characterization of GDP-hexose phosphorylase activities of recombinant human C15orf58 and *C. elegans* C10F3.4 proteins

K_m and V_{max} values were obtained by fitting the experimental data to the Michaelis-Menten equation using the K_m calculator of the BioMechanic program. Enzymatic turnover numbers were derived from the V_{max} values by using a molecular mass of 45 and 55.7 kDa for His-tagged C15orf58 and C10F3.4, respectively, with the assumption that the enzyme preparations were pure. Incubation times and enzyme concentrations were adjusted to obtain initial velocity data. Enzymatic activities were measured by the HPLC assay described under "Experimental Procedures" except for the GDP-D-Glc phosphorylase activity of the *C. elegans* enzyme where the spectrophotometric assay described under "Experimental Procedures" was used. The worm and human recombinant enzymes were assayed at 26 and 31 °C, respectively. K_m and V_{max} values for the GDP-hexoses were obtained in the presence of 5 mM inorganic phosphate, whereas those for inorganic phosphate were obtained in the presence of 50 μM GDP-D-Glc. Values are the means ± S.D. calculated from three to five individual experiments for each substrate except for inorganic phosphate for which the kinetic parameters of the human enzyme were only determined twice.

Substrate	k_{cat}		K_m		k_{cat}/K_m	
	Human	*C. elegans*	Human	*C. elegans*	Human	*C. elegans*
	s^{-1}		mM		$s^{-1}\ M^{-1}$	
GDP-D-Glc	26.0 ± 7.4	265 ± 15	0.0020 ± 0.0009	0.010 ± 0.004	$1.5 \pm 0.8 \times 10^7$	$3.0 \pm 1.2 \times 10^7$
GDP-D-Man	2.1 ± 0.2	0.89 ± 0.37	0.042 ± 0.003	0.33 ± 0.16	$4.9 \pm 0.7 \times 10^4$	$2.9 \pm 0.4 \times 10^3$
GDP-L-Gal	5.1 ± 0.3	0.40 ± 0.28	0.012 ± 0.002	0.011 ± 0.008	$4.3 \pm 0.9 \times 10^5$	$4.0 \pm 1.8 \times 10^4$
Inorganic phosphate	28.1 ± 0.1	380 ± 27	2.9 ± 0.6	1.2 ± 0.2	$9.9 \pm 2.1 \times 10^3$	$312 \pm 37 \times 10^3$

were measured by HPLC-based methods that simultaneously monitor the consumption of GDP-D-Glc and the formation of the possible products (GMP, GDP, GTP, GDP-L-Gal, and GDP-D-Man, respectively). Despite the replacement of the Gln residue of the VTC2 HIT motif by a His residue in the HIT motifs of the human and worm proteins, the latter did not hydrolyze GDP-D-Glc. In fact, as for the VTC2 enzyme, the human and worm VTC2 homologs only acted on GDP-D-Glc in the presence of P_i (supplemental Fig. S1), and GDP-D-Glc consumption was accompanied by a concomitant formation of stoichiometric amounts of GDP (data not shown). These results showed that the mammalian and invertebrate VTC2 homologs are, like the plant enzyme, HIT nucleotide phosphorylases and not hydrolases.

We then determined the kinetic parameters of these human and worm phosphorylases for GDP-D-Glc, GDP-D-Man, and GDP-L-Gal using the HPLC and/or the spectrophotometric assays described under "Experimental Procedures" (Table 1). For both enzymes, we found low micromolar K_m values and high catalytic efficiencies with GDP-D-Glc as a substrate. As opposed to plant VTC2, which phosphorolyzes GDP-D-Glc and GDP-L-Gal with similar catalytic efficiencies (1), the catalytic efficiencies of the human and worm enzymes for GDP-L-Gal were 35- and 750-fold lower, respectively, than for GDP-D-Glc. GDP-D-Man was, as for plant VTC2 (1), a poor substrate for the human and worm phosphorylases. Also, as for plant VTC2 (24), affinities in the low millimolar range were found with the human and worm enzymes for the nucleotide acceptor P_i. These results show that the human C15orf58 and worm C10F3.4 proteins act as specific and highly efficient GDP-D-Glc phosphorylases. The enzymatic activity of C10F3.4 was also measured in the reverse direction by incubating the protein in the presence of D-Glc-1-P and GDP, ADP, UDP, or CDP and assaying NDP-D-Glc formation in the absence of added P_i (supplemental Table S1). Significant NDP-D-Glc formation was measured in these reactions in the presence of GDP. More than 10-fold lower activities were detected in the presence of UDP, and no activity was found in the presence of CDP. Relatively high ADP-D-Glc levels were measured after incubating D-Glc-1-P in the presence of ADP, but this reaction was not dependent on the presence of the C10F3.4 enzyme (supplemental Table S1). These results demonstrate the specificity of the enzyme for the guanosine nucleotide at least in the presence of D-Glc-1-P.

The high substrate affinity of C15orf58 and C10F3.4 for GDP-D-Glc made it relatively difficult to accurately determine the kinetic parameters of their GDP-D-Glc phosphorylase activity by the HPLC method; the product (GDP) concentrations to be measured under initial velocity conditions at GDP-D-Glc concentrations below and around the K_m values of these enzymes for GDP-D-Glc were close to the detection limit of the assay. We therefore developed an enzymatic spectrophotometric assay to monitor D-Glc-1-P formation from GDP-D-Glc by coupling this reaction to those catalyzed by phosphoglucomutase and glucose-6-P dehydrogenase in the presence of NAD^+. In this assay, the D-Glc-1-P formed is successively converted to D-Glc-6-P and then to 6-phospho-D-glucono-δ-lactone with concomitant reduction of NAD^+ to NADH, which is detected by its UV absorbance at 340 nm. The K_m values for GDP-D-Glc obtained by this method for C15orf58 and C10F3.4 (3.4 ± 1.0 and 10 ± 4 μM, respectively) were similar to the values obtained with the HPLC method (2.0 ± 0.9 and 18 ± 11 μM, respectively). Similar k_{cat} values were also obtained for GDP-D-Glc with human C15orf58 using the spectrophotometric assay (16 ± 0.4 s^{-1}) and the HPLC method (26 ± 7 s^{-1}). However, using the HPLC method, a non-Michaelis-Menten decrease in activity was observed at higher GDP-D-Glc concentrations with the worm C10F3.4 enzyme (but not with the human C15orf58 enzyme). This inhibitory effect was not observed using the spectrophotometric assay, suggesting that it might be due to product inhibition and making the spectrophotometric assay our preferred method for kinetic analyses of the GDP-D-Glc phosphorylase activity of C10F3.4. Furthermore, the use of these two different methods allowed us to confirm the identity of the two products formed by the P_i-dependent conversion of GDP-D-Glc by C15orf58 and C10F3.4 as D-Glc-1-P (spectrophotometric assay) and GDP (HPLC method).

GDP-D-Glc Phosphorylase Activity in Mouse Tissue and Worm Extracts—GDP-D-Glc phosphorylase activity was also detected in mouse tissue and *C. elegans* extracts. The activity levels measured in these extracts as the P_i-dependent GDP formation from GDP-D-Glc (0.5–3 nmol min^{-1} mg of $protein^{-1}$; see Table 2 and Figs. 1 and 3) were of the same magnitude as the GDP-L-Gal phosphorylase activity measured in *Arabidopsis* whole plant extracts (24). Under the assay conditions described under "Experimental Procedures," GDP formation measured in the desalted protein extracts in the presence of GDP-D-Glc but

in the absence of externally added Pi was low (less than 0.2 nmol min^{-1} mg of $protein^{-1}$). Recapitulating the substrate specificity for the recombinant C15orf58 and C10F3.4 proteins, a preference for GDP-D-Glc over GDP-L-Gal and GDP-D-Man was also found in mouse brain extracts (Table 2) and in *C. elegans* extracts (supplemental Table S2) when measuring P_i-dependent GDP formation from these GDP-hexoses. No (or very low) phosphorylase activities were detected for human C15orf58 (Table 2) or worm C10F3.4 (supplemental Table S2) recombinant proteins with other NDP-hexoses including GDP-L-Fuc, UDP-D-Glc, UDP-D-Gal, and ADP-D-Glc. Similarly, little or no phosphorylase activity toward GDP-L-Fuc, UDP-D-Glc, UDP-D-Gal, and ADP-D-Glc was detected in mouse brain extracts (Table 2) and *C. elegans* extracts (supplemental Table S2).

TABLE 2

Comparison of substrate specificity of human recombinant C15orf58 and of mouse brain GDP-D-Glc phosphorylase

Various sugar nucleotides (50 μM) were incubated in the presence of C15orf58 recombinant enzyme (0.011 μg/ml) for 25 min or of desalted mouse brain extracts (0.3–0.5 mg of protein/ml) for 20 min at 31 °C. NDP-hexose consumption and NDP production were measured by HPLC as described under "Experimental Procedures." Phosphorylase activities were calculated based on the P_i-dependent NDP formation. With GDP-D-Glc as a substrate, the specific activity of the human recombinant C15orf58 enzyme was 29.4 ± 3.2 μmol min^{-1} mg of $protein^{-1}$ (100%); the corresponding 100% specific activity of the mouse brain extract was 1.9 ± 0.7 nmol min^{-1} mg of $protein^{-1}$ (specific activities are means ± S.D., $n = 2$). The phosphorylase activities found with the other sugar nucleotides are given as a percentage of the activity found with GDP-D-Glc. Values represent the means of two individual experiments for each substrate.

Substrate	Relative specific activity	
	Recombinant human enzyme	Mouse brain extract
	%	
GDP-D-Glc	100	100
GDP-L-Gal	23	27
GDP-D-Man	2	5
GDP-L-Fuc	0	0
UDP-D-Glc	1	5
UDP-D-Gal	0	3
ADP-D-Glc	0	1

These results indicate that mammalian and worm tissues contain a GDP-D-Glc phosphorylase activity with properties similar to those of the recombinant C15orf58 and C10F3.4 enzymes.

Confirmation of Identity of C10F3.4 and C15orf58 as C. elegans and Human GDP-D-Glc Phosphorylases—To confirm that the human and *C. elegans* GDP-D-Glc phosphorylases are encoded by the *C15orf58* and *C10F3.4* genes, respectively, we measured this enzymatic activity in extracts of cells where the expression of these genes was eliminated or reduced. We used a mutant *C. elegans* strain (*tm2679*) that has a 444-bp deletion within the *C10F3.4* gene. This deletion eliminates exons 6 to 7 and parts of exons 5 and 8 and introduces a premature stop codon. The mutated allele encodes a predicted truncated 246-amino acid protein that lacks the C-terminal moiety of the 458-amino acid wild-type C10F3.4 protein (isoform a). Whereas GDP-D-Glc phosphorylase activity could readily be measured in wild-type *C. elegans* extracts, no such activity could be detected in extracts prepared from mutant *tm2679* worms (Fig. 1*A*). These mutant worms, however, did not present any apparent abnormal phenotype in the standard culture conditions used throughout this study.

For the human enzyme, we knocked down the *C15orf58* gene in HEK293T cells by transfection with an siRNA pool specifically targeting this gene. As shown in Fig. 1*B*, a reduction of about 50% in *C15orf58* transcript level was obtained in cells treated with *C15orf58* siRNAs compared with cells treated with non-targeting control siRNA. This decrease in mRNA expression level was accompanied by an ~2-fold decrease in GDP-D-Glc phosphorylase activity in extracts derived from these cells (Fig. 1*B*). These findings establish the molecular identity of the *C. elegans* and human GDP-D-Glc phosphorylases as corresponding to the expression products of the *C10F3.4* and *C15orf58* genes, respectively.

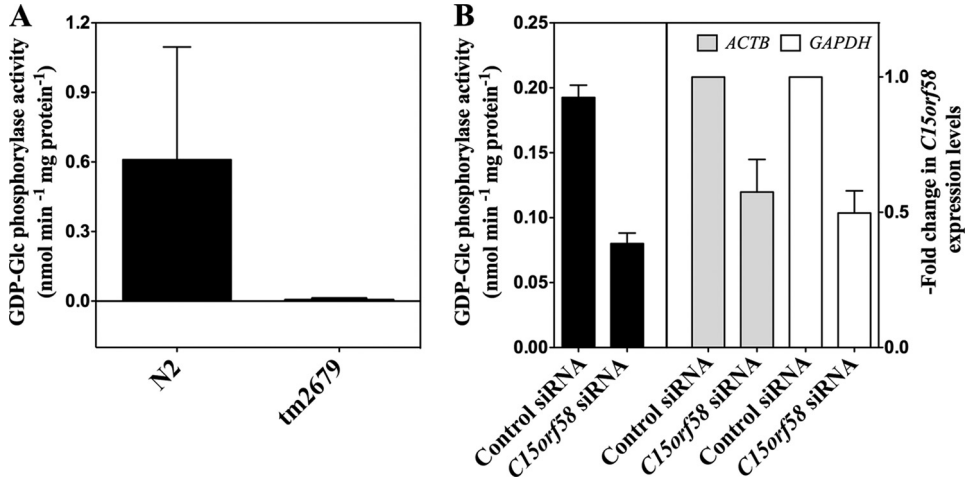

FIGURE 1. **GDP-D-Glc phosphorylase activity in *C. elegans C10F3.4* deletion strain and in HEK293T cells treated with *C15orf58* siRNA.** Extracts were prepared from wild-type (N2) or *C10F3.4* mutant (*tm2679*) *C. elegans* strains (*A*) and from siRNA-transfected HEK293T cells (*B*), and GDP-D-Glc phosphorylase activity was measured by the HPLC assay described under "Experimental Procedures." GDP-D-Glc was added to the reaction mixtures at a final concentration of 50 μM. The worm and HEK293T cell extracts were diluted in the reaction mixtures to final protein concentrations of 0.5–1.4 and 0.3–0.4 mg/ml, respectively. Control reactions were run in the absence of sodium phosphate, and GDP-D-Glc phosphorylase activities were calculated based on the P_i-dependent formation of GDP. *A*, worms were grown for 4–7 days at 20 °C in liquid culture and harvested for protein extraction. *B*, HEK293T cell cultures were stopped 48–72 h after siRNA transfection. In addition to GDP-D-Glc phosphorylase activity assays (*black bars*), quantitative RT-PCR was performed on cDNA derived from these cells. *C15orf58* mRNA levels were normalized to those of *ACTB* (*β*-actin; *gray bars*) or *GAPDH* (*white bars*), and -fold changes in *C15orf58* expression in knockdown *versus* control cells were calculated using the 2^{-ddCt} method. The results shown represent the means ± S.D. of two to three (*A*) or four (*B*) biological replicates.

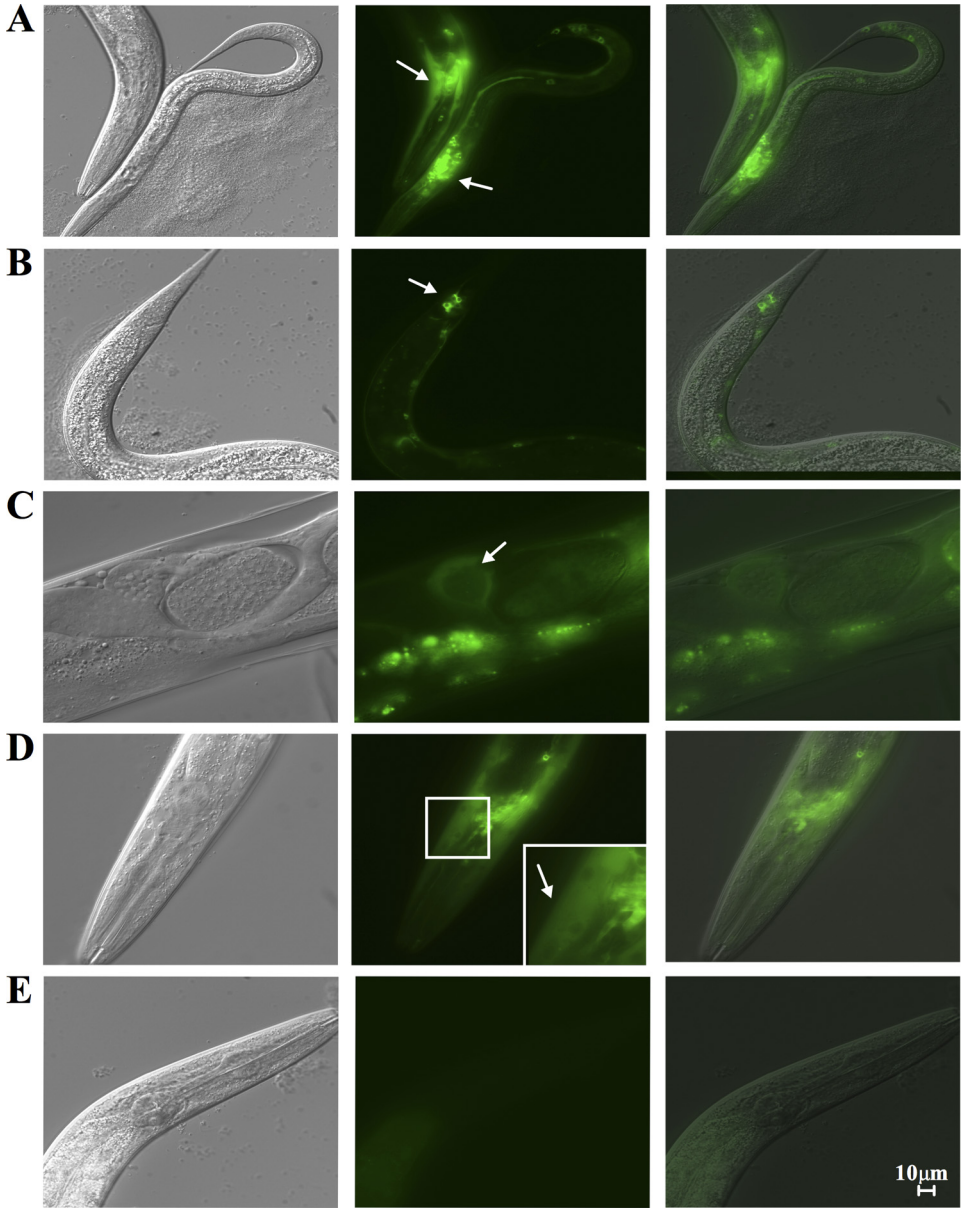

FIGURE 2. **C10F3.4 expression pattern in *C. elegans*.** A transgenic *C. elegans* strain (*UZ119*) expressing a C10F3.4::GFP fusion protein was generated as described under "Experimental Procedures." The differential interference contrast images are presented in the *left panels*, GFP images are in the *middle panels*, and merged images are in the *right panels*. C10F3.4::GFP expression is seen in head neurons (*arrows*) (*A*), in neuronal cells throughout the ventral nerve cord and in tail (lumbar) ganglia (*arrow*) (*B*), in the spermatheca (*arrow*) (*C*), and in anterior hypodermis cells (*arrow* in *inset* representing a magnified region) (*D*). The *bottom panels* show a worm that lost the extrachromosomal array containing the C10F3.4::GFP transgene (*E*, negative control). Transgenic animals were analyzed for GFP expression at 40× power *magnification*.

Tissue Distribution of C. elegans and Mouse GDP-D-Glc Phosphorylases—As a first step in elucidating the physiological role of the GDP-D-Glc phosphorylase enzyme in worm and mammalian tissues, we determined the tissue distribution of this protein in live worms as well as of the corresponding activity in mouse extracts. A transgenic *C. elegans* strain (*UZ119*) expressing a C10F3.4::GFP fusion protein under the endogenous *C10F3.4* promoter was used to determine in which cell types and tissues this protein is expressed in nematodes. Remarkably, significant expression of this protein seemed to be mostly confined to neurons and parts of the reproductive system. As shown in Fig. 2, cytosolic expression of the C10F3.4 protein was detected throughout the neuronal system. In addition, expression was observed in the spermatheca and in anterior hypodermal cells. The high neuronal expression was found in all the normal larval stages observed. C10F3.4 expression was also detected in developing embryos.

To examine the tissue distribution of the GDP-D-Glc phosphorylase in mammals, we measured enzyme activity in extracts of various mouse tissues. All of the analyzed tissues contained GDP-D-Glc phosphorylase activity, but the highest levels were reproducibly measured in brain and testis (4–8 times higher activities than in the remaining tissues; Fig. 3). We also measured mRNA expression of the *C15orf58* gene (designated *D330012F22Rik* in mouse) in various mouse tissues using real time quantitative PCR. The mRNA distribution pattern revealed an up-regulation of the mouse *C15orf58* homolog mRNA in brain and testis relative to kidney, liver, and heart

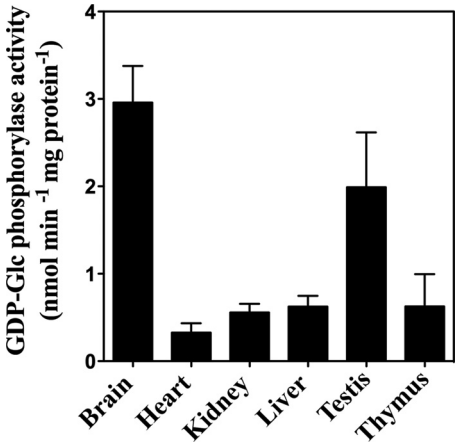

FIGURE 3. **Tissue distribution of GDP-D-Glc phosphorylase activity in mouse.** Mouse tissue extracts were prepared, and GDP-D-Glc phosphorylase activities were measured by HPLC as described under "Experimental Procedures." GDP-D-Glc and mouse tissue extracts were added to the reaction mixtures at final concentrations of 50 μM and 0.3–1.5 mg of protein/ml, respectively. Control reactions were run in the absence of sodium phosphate, and GDP-D-Glc phosphorylase activities were calculated based on the P_i-dependent formation of GDP. The results shown represent the means ± S.D. of three to five biological replicates.

(supplemental Fig. S2), thus supporting the distribution pattern obtained via GDP-D-Glc phosphorylase activity measurements. Taken together, these results also demonstrated that, in addition to displaying similar substrate specificity and kinetic properties, the *C. elegans* and mammalian GDP-D-Glc phosphorylases share similar expression profiles with highest occurrence in the nervous and male reproductive systems.

GDP-D-Glc Is Present at Low Levels in Nematode and Mouse Tissues but Accumulates in Absence of GDP-D-Glc Phosphorylase—Data on the presence and formation of GDP-D-Glc in living organisms are scarce, but GDP-D-Glc has been isolated from mammary gland (7). Furthermore, a GDP-D-Glc pyrophosphorylase activity, forming GDP-D-Glc from GTP and D-Glc-1-P in the reverse reaction, has been measured in extracts prepared from various mammalian (7, 8) and plant sources (25). Although this activity could be clearly distinguished from UDP-D-Glc pyrophosphorylase, it has most often been found in association with GDP-D-Man pyrophosphorylase activity (8–10) and may thus result from a lack of substrate specificity of the enzyme that forms GDP-D-Man for glycoconjugate synthesis. We thus developed methods to directly measure GDP-D-Glc and GDP-D-Man in cell extracts.

We first set up a specific and sensitive assay of these GDP-hexoses that was adapted from a previously published ion pair liquid chromatography coupled to electrospray ionization mass spectrometry method (21) as described under "Experimental Procedures." This method allowed us to distinguish between GDP-D-Man and GDP-D-Glc both by elution time and by the relative abundance of product ions m/z 604 → 158 and m/z 604 → 362 (both generated from the common precursor ion m/z 604) (Fig. 4*A*). GDP-D-Man reproducibly eluted earlier from the LC column than GDP-D-Glc and consistently generated higher levels of product ion 604 → 158 than of product ion 604 → 362 in the range of GDP-D-Man concentrations analyzed. GDP-D-Glc on the other hand generated higher levels of the product ion 604 → 362. The 158/362 product ion peak intensity ratio found for GDP-D-Man and GDP-D-Glc corresponded to 3.4 and 0.13, respectively, over the range of GDP-hexose concentrations analyzed in this study by the IP-LC-ESI-MS method. For quantification, standard curves were generated for GDP-D-Man and GDP-D-Glc by injecting 10–100 and 0.1–4 pmol of these compounds, respectively, in a volume of 10 μl and by determining the corresponding product ion 604 → 158 (GDP-D-Man) and 604 → 362 (GDP-D-Glc) peak areas of the extracted ion current (supplemental Fig. S3). We found that amounts of GDP-D-Glc corresponding to as low as 0.05 pmol could readily be detected by this method.

We then quantified GDP-D-Man and GDP-D-Glc in neutralized perchloric acid extracts prepared from wild-type (N2) and *tm2679* mutant *C. elegans* worms grown in liquid culture and from a series of mouse tissues as described under "Experimental Procedures" (Table 3). Similar amounts of GDP-D-Man were found in *tm2679* and N2 worms (7.7 *versus* 8.9 nmol/g of worms), whereas more than 5-fold higher amounts of GDP-D-Glc were detected in the *C10F3.4* deletion strain *versus* wild-type worms (0.11 *versus* 0.02 nmol/g of worms). It should be noted that the GDP-D-Glc levels found in wild-type worms were actually close to the detection limit of our assay. This observation indicated that the best substrate found *in vitro* for the C10F3.4 phosphorylase is a physiological substrate for this enzyme in worms. Concerning wild-type mouse tissues, GDP-D-Man concentrations varying from about 7 to 25 nmol/g of tissue (wet weight) were measured; liver was the organ with the highest levels of this GDP-hexose (Table 3). These values were similar to GDP-D-Man concentrations found previously in rat tissues (26). GDP-D-Glc levels were very low in all of the mouse tissues analyzed. The highest GDP-D-Glc levels were measured in liver (0.15 nmol/g of tissue) where GDP-D-Glc concentrations were found to be more than 100-fold lower than GDP-D-Man concentrations. The GDP-D-Glc levels detected in brain, kidney, testis, and heart were 15–30-fold lower than in liver. Except for liver, all of the GDP-D-Glc levels found in mouse tissues were near or below the detection limit of our assay. Taken together, these results suggest that GDP-D-Glc levels are normally maintained at very low levels in cells. The only situation in which we found more significant GDP-D-Glc levels was in extracts of a *C. elegans* mutant of the C10F3.4 GDP-D-Glc phosphorylase activity. We conclude that a physiological function of GDP-D-Glc phosphorylase in nematode cells is to degrade GDP-D-Glc to D-Glc-1-P and hypothesize that such an activity is needed to prevent misincorporation of glucose for mannose into glycoconjugates (Fig. 5). The situation in mammalian cells may be similar.

DISCUSSION

In an effort to understand the function of apparent orthologs of the plant VTC2 enzyme in non-plant organisms, we found that *C. elegans* and mammalian tissues contain a specific GDP-D-Glc phosphorylase enzyme encoded by the *C10F3.4* gene in worms and the *C15orf58* gene in humans. As opposed to the plant VTC2 enzyme, the C10F3.4 and C15orf58 proteins display a marked preference for GDP-D-Glc over GDP-L-Gal as a substrate. However, like the VTC2 enzyme, the C10F3.4 and C15orf58 enzymes are also completely dependent on the pres-

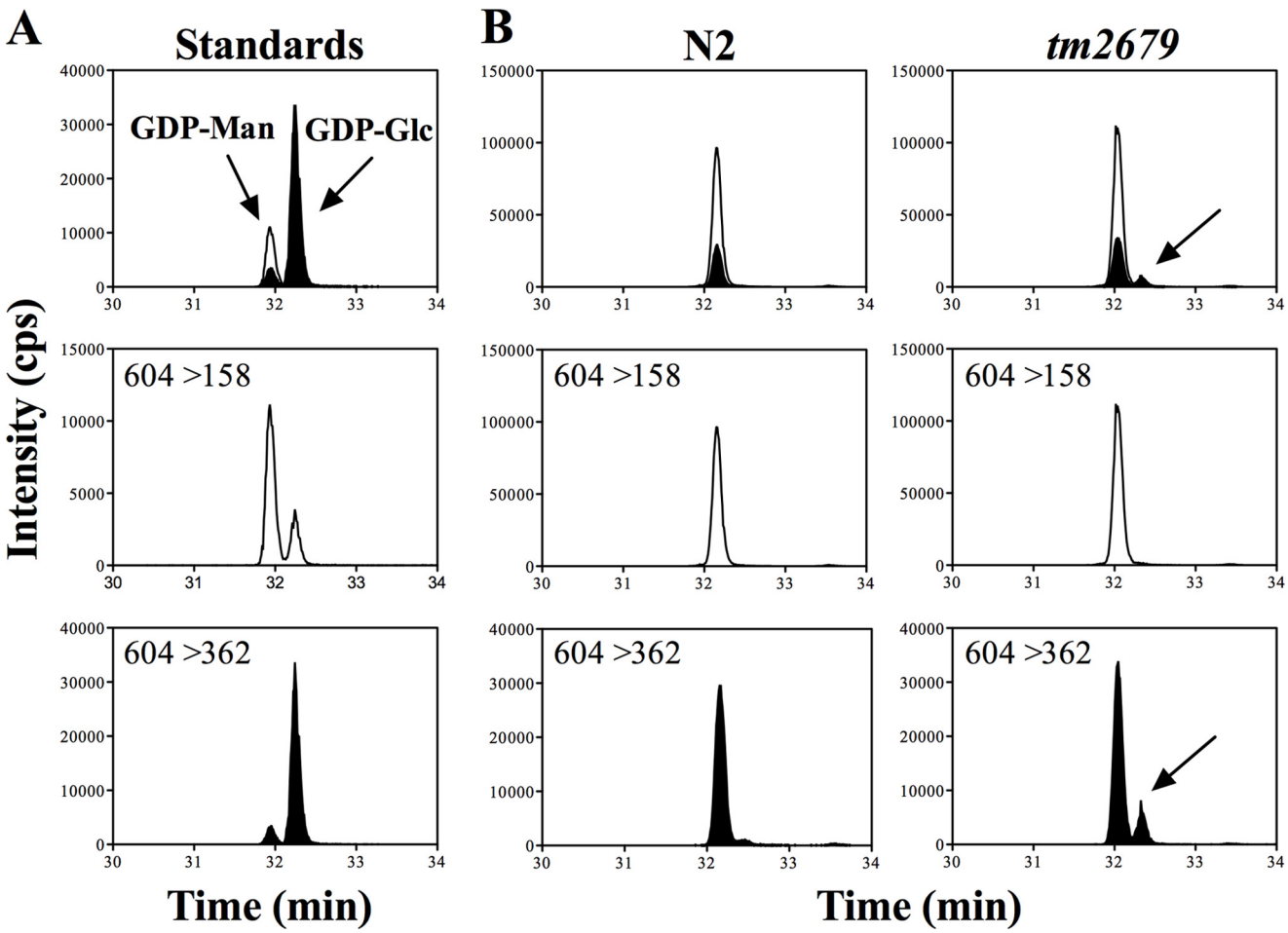

FIGURE 4. **Accumulation of GDP-D-Glc in *C10F3.4* mutant *C. elegans* strain (*tm2679*).** GDP-D-Man and GDP-D-Glc standards (*A*) and wild-type N2 and mutant *tm2679* small molecule extracts (*B*) were analyzed by the IP-LC-ESI-MS method described under "Experimental Procedures." *A*, extracted ion chromatograms of product ions *m/z* 604 → 158 (*middle panel*, *white area*) and *m/z* 604 → 362 (*bottom panel*, *black area*) obtained after injection of a solution containing 0.2 pmol of GDP-D-Man and 0.2 pmol of GDP-D-Glc. GDP-D-Man and GDP-D-Glc produced the same precursor ion, *m/z* 604, and the same product ions, *m/z* 604 → 158 and *m/z* 604 → 362. These GDP-hexoses, however, displayed different retention times with GDP-D-Man eluting first and different relative peak intensities for the product ions. The *top panel* shows an overlay of the extracted ion chromatograms of product ions *m/z* 604 → 158 (*white area*) and *m/z* 604 → 362 (*black area*) presented separately in the *middle* and *bottom panels*. *B*, extracted ion chromatograms of product ions *m/z* 604 → 158 (*middle panels*, *white areas*) and *m/z* 604 → 362 (*bottom panels*, *black areas*) after injection of equal volumes of *C. elegans* N2 and *tm2679* perchloric acid extracts. The *top panels* show overlays of the corresponding *middle* and *bottom panels*. The *arrows* indicate the peak identified as GDP-D-Glc and accumulating in *C10F3.4* mutant worms. Representative chromatograms obtained with one set of wild-type and mutant extracts are shown. Four other sets of wild-type and *tm2679* mutant extracts were analyzed with similar results. The GDP-D-Man and GDP-D-Glc levels found in these worm extracts were quantified, and the values obtained are given in Table 3. *cps*, counts/s.

ence of inorganic phosphate to act on GDP-D-Glc, thereby converting it into D-Glc-1-P and GDP. The identity of the reaction products was confirmed by HPLC (for GDP) and by an enzymatic spectrophotometric assay (for D-Glc-1-P).

The P_i dependence of the C10F3.4 and C15orf58 enzymes was somewhat unexpected given that the Gln residue of the VTC2 "HIT motif" (H*X*H*X*Q) was replaced by a His residue in the HIT motifs of both the worm and human VTC2 homolog sequences (H*X*H*X*H). So far, the H*X*H*X*H motif has been proposed to be characteristic of HIT nucleotide hydrolases, whereas the H*X*H*X*Q motif has been considered as predictive of a nucleotide transferase or phosphorylase activity (11, 12). The present study and two other recent reports indicate that this "rule" has exceptions. In addition to C10F3.4 and C15orf58, a mycobacterial protein (Rv2613c) containing a H*X*H*X*H motif has also recently been reported to act as a phosphorylase (on diadenosine tetraphosphate) and not as a hydrolase (27). Furthermore, *A. thaliana* Hint4 and *C. elegans* DcpS, two HIT proteins containing the H*X*H*X*H motif, have been shown to display a phosphorolytic activity toward adenosine 5′-phosphosulfate in addition to their hydrolytic activity on this substrate (28). The phosphorylase activity of the latter two enzymes, however, was minor compared with their hydrolase activity at neutral pH. Taken together, these results suggest that critical residues other than the C-terminal residue of the HIT motif (His or Gln) must be involved in determining whether the nucleotidylated enzyme intermediate that is formed during HIT enzyme-catalyzed reactions is resolved via hydrolysis or phosphorolysis.

Concerning the nucleotide moiety of the nucleotide sugar substrate, recombinant C10F3.4 and C15orf58 appear to be specific for GDP as none of the ADP- or UDP-hexoses tested were phosphorolyzed by either of these proteins and as GDP could not be replaced in the reverse reaction by ADP, UDP,

TABLE 3

GDP-D-Man and GDP-D-Glc levels in *C. elegans* and various mouse tissues

GDP-D-Man and GDP-D-Glc levels were determined in neutralized perchloric acid extracts of wild-type (N2) and *C10F3.4* mutant (*tm2679*) worms as well as of various mouse tissues by using the IP-LC-ESI-MS method described under "Experimental Procedures." GDP-hexose concentrations were determined based on peak areas of selected product ions (604 → 362 for GDP-D-Glc and 604 → 158 for GDP-D-Man) and calibration curves established with standard GDP-D-Man and GDP-D-Glc solutions. Metabolite concentrations were normalized against wet worm or mouse tissue weight. Values are means ± S.D. of five (*C. elegans*) or two (mouse tissue) biological replicates. Statistical analysis using a two-tailed unpaired Student's *t* test shows a statistically significant difference in GDP-D-Glc concentration and GDP-D-Glc/GDP-D-Man ratio between the N2 and *tm2679 C. elegans* strains as demonstrated by the indicated *p* values.

	C. elegans		
Strain	**GDP-D-Man**	**GDP-D-Glc**	**GDP-Glc/GDP-Man**
	nmol/g worms	*nmol/g worms*	$\times 10^{-3}$
N2	8.9 ± 5.4	0.020 ± 0.009	2.3 ± 0.7
tm2679	7.7 ± 4.6	0.11 ± 0.07 ($p = 0.029$)	13.8 ± 2.2 ($p = 0.000004$)
	Mouse		
Tissue	**GDP-D-Man**	**GDP-D-Glc**	**GDP-Glc/GDP-Man**
	nmol/g tissue	*nmol/g tissue*	$\times 10^{-3}$
Liver	25 ± 2	0.15 ± 0.01	6.1 ± 0.1
Brain	13 ± 0.2	0.0077 ± 0.0012	0.6 ± 0.02
Kidney	6.8 ± 0.4	0.0096 ± 0.0002	1.4 ± 0.06
Testis	11 ± 0.1	0.0052 ± 0.0016	0.48 ± 0.14
Heart	7.8 ± 0.5	0.0055 ± 0.0018	0.70 ± 0.27

or CDP for transfer to D-Glc-1-P. As to the sugar moiety of the GDP-sugar substrate, the C10F3.4 and C15orf58 enzymes displayed a marked preference for D-Glc over L-Gal, D-Man, and L-Fuc. A similar substrate specificity was found for the GDP-hexose phosphorylase activity detected in *C. elegans* and mouse tissue extracts. This finding as well as the absence of GDP-D-Glc phosphorylase activity in mutant worms lacking a functional *C10F3.4* gene and decreased GDP-D-Glc phosphorylase activity in *C15orf58* siRNA knockdown human cells led us to conclude that *C10F3.4* and *C15orf58* encode for the *C. elegans* and human GDP-D-Glc phosphorylase enzymes, respectively.

A link of the mammalian VTC2 homolog to vitamin C synthesis seemed very unlikely because mammals (except for a few non-ascorbate-synthesizing species including humans) synthesize ascorbate via a pathway that is different from the plant pathway and that does not involve GDP-L-Gal as an intermediate (6). However, the presence of a *VTC2*-homologous gene in *C. elegans* raised questions concerning a possible existence of a plant-like ascorbate biosynthesis pathway in this species. The finding that the C10F3.4 enzyme was more than 700-fold less efficient in phosphorolyzing GDP-L-Gal than GDP-D-Glc, however, was a first indication that this enzyme is not likely to participate in a plant-like vitamin C synthesis pathway in *C. elegans*. Interestingly, we could actually detect significant amounts of ascorbate in *C. elegans* worms, but similar levels were found in wild-type and *C10F3.4* mutant worms,[5] again arguing against C10F3.4 involvement in ascorbate formation in worms. Combining these observations with the absence of any obvious orthologs of critical enzymes of the plant vitamin C biosynthesis pathway (*e.g.* GDP-D-mannose 3,5-epimerase and L-galactonolactone dehydrogenase) in *C. elegans* (1), we conclude that if ascorbate is formed in this species it is not via a plant-like L-galactose pathway involving the C10F3.4 enzyme.

Our characterization of the substrate specificity and kinetic properties of the C10F3.4 and C15orf58 proteins and the observed accumulation of GDP-D-Glc in C10F3.4-deficient worms indicate that GDP-D-Glc is a physiological substrate of these enzymes. Why would invertebrates and vertebrates have conserved an enzyme that breaks down GDP-D-Glc into D-Glc-1-P and GDP? The literature on GDP-D-Glc is scarce, but the presence of this GDP-hexose was reported in the early 1960s in lactating bovine mammary gland (7), and an enzymatic activity forming GDP-D-Glc from GTP and D-Glc-1-P (GDP-D-Glc pyrophosphorylase) has also been found in various plant (25) and animal tissues (8, 9). At least in mammals, however, this activity has so far always been found in association with GDP-D-Man pyrophosphorylase. Nothing is known about possible functions of GDP-D-Glc in mammals or invertebrates, but GDP-D-Glc acts as a glucosyl donor for the synthesis of cell wall polysaccharides in various plant species (29–32) and for trehalose synthesis in certain bacterial species (33).

Mammalian GDP-D-Man pyrophosphorylase has been purified from rat mammary gland and calf liver (8), from pig thyroid (34), and from pig liver (9). Although the thyroid enzyme was specific for GDP-D-Man, both the mammary gland and liver enzymes have been shown to use GDP-D-Man as well as GDP-D-Glc as substrates. Remarkably, the native pig liver enzyme was actually about 2 times more active in forming GDP-D-Glc than in the synthesis of GDP-D-Man (10). This enzyme is composed of two different subunits (α- and β-subunits) encoded by two different genes. Only the gene encoding the β-subunit has so far been cloned and expressed (10). The expression product of this gene was shown to be a functional GDP-D-Man pyrophosphorylase that, unlike the native enzyme, is about 6 times more active in forming GDP-D-Man than GDP-D-Glc. Based on this, it was suggested that the α-subunit could be the GDP-D-Glc pyrophosphorylase or a regulatory subunit that affects the substrate specificity of the β-subunit. It is of interest to note here that genes encoding homologs of the α- and β-subunits of GDP-D-Man pyrophosphorylase are also found in the *C. elegans* genome. On the contrary, no gene encoding an α-subunit is found in the genome of *Saccharomyces cerevisiae*, and the GDP-D-Man pyrophosphorylase of this species, which presents high similarity with mammalian GDP-D-Man pyrophosphorylase β, has been reported to be quite specific for GDP-D-Man (10). The *S. cerevisiae* genome does not encode a VTC2 homolog either. Taken together, these results suggest a link between the formation of GDP-D-Glc by a second activity of the enzyme that normally makes GDP-D-Man and the presence of a GDP-D-Glc phosphorylase that specifically degrades the glucose-containing nucleotide sugar. In favor of this, we found a similar tissue distribution pattern of GDP-D-Glc phosphorylase and GDP-D-Man pyrophosphorylase α (Gmppa) at the mRNA level in mice (supplemental Fig. S2).

GDP-D-Man is the major mannosyl donor for the synthesis of *N*-linked glycoproteins and glycosylphosphatidylinositol membrane anchors (35). It is also the precursor of GDP-

[5] B. D. Young and L. N. Adler, unpublished results.

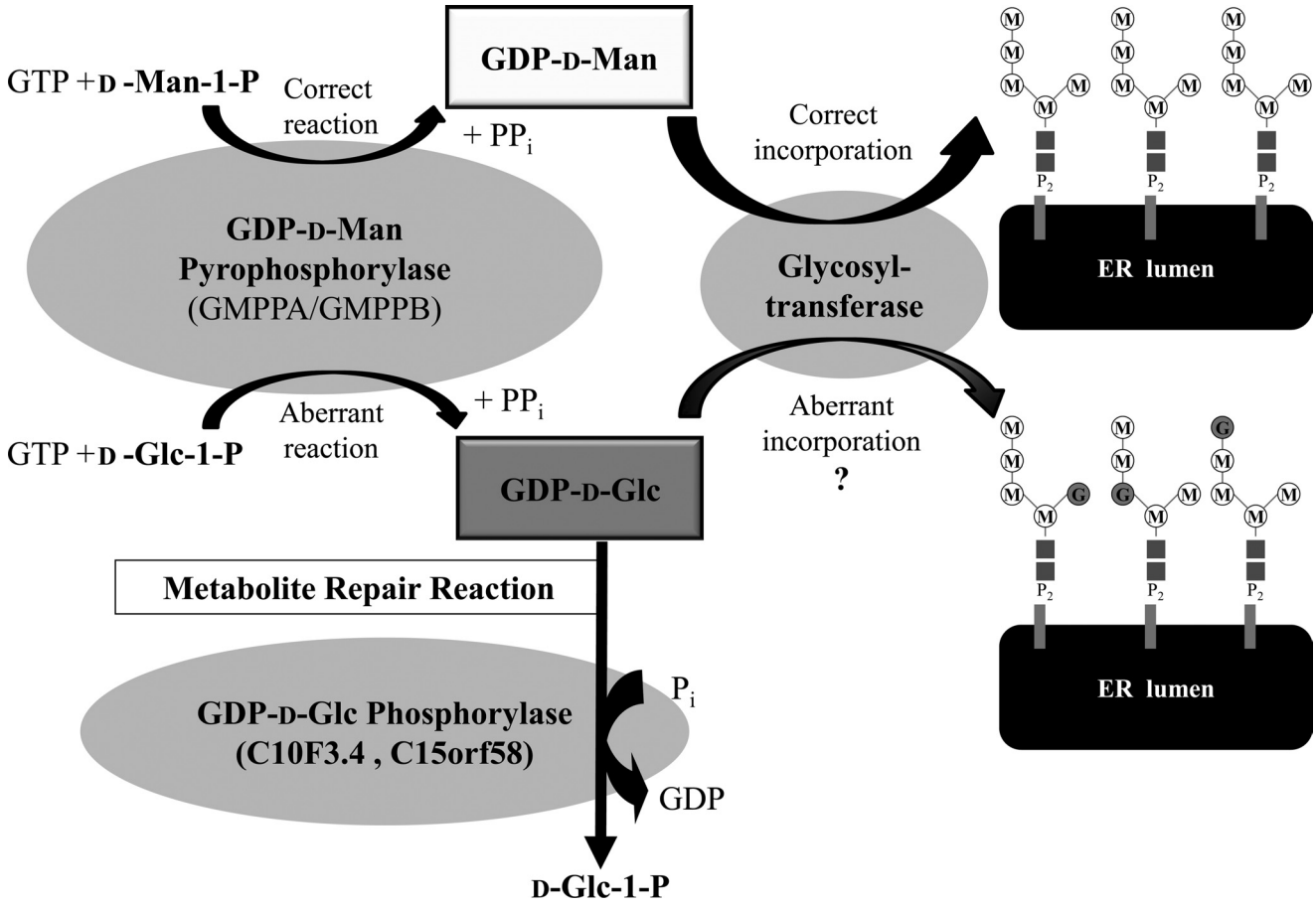

FIGURE 5. **Possible role of GDP-D-Glc phosphorylase in preventing misincorporation of glucose in place of mannose residues into glycoconjugates.** In the presence of GTP and D-Man-1-P, GDP-D-Man pyrophosphorylase forms GDP-D-Man, a major mannosyl donor for glycoconjugation. The native pyrophosphorylase is composed of α- and β-subunits (GMPPA and GMPPB) and has been shown to also catalyze the formation of GDP-D-Glc when D-Man-1-P is replaced by D-Glc-1-P. However, we show in this study that mammalian tissues contain only very low levels of GDP-D-Glc. In addition, this nucleotide sugar accumulates in mutant worms lacking GDP-D-Glc phosphorylase, the enzyme described in the present work. We therefore propose that GDP-D-Glc phosphorylase functions to compensate for the lack of specificity of GDP-D-Man pyrophosphorylase by degrading the apparently useless GDP-D-Glc. This may be important to prevent misincorporation of glucose residues for mannose residues into oligosaccharide chains such as those linked to dolichol (this figure) and eventually transferred to proteins. GDP-D-Glc phosphorylase might thus be necessary to preserve functional protein *N*-glycosylation or other glycoconjugation processes. *ER*, endoplasmic reticulum.

L-Fuc, another important glycosyl donor for glycoprotein biosynthesis (35). In various bacterial, lower eukaryotic, and plant species, GDP-D-Man donates mannosyl residues for cell wall polysaccharides (32, 36, 37). Given the close structural similarity of GDP-D-Man and GDP-D-Glc (they only differ by the configuration of their hydroxyl group on C2 of the sugar moiety), it can be hypothesized that some of the enzymes using GDP-D-Man are not entirely specific for their substrate and can use GDP-D-Glc instead (or be competitively inhibited by the latter). In favor of this, glycosyltransferases that use nucleotide sugars as the glycosyl donors seem to be often particularly specific for the nucleotide portion of their substrate while having some tolerance for different sugars (38). This lack of specificity could be indirectly corrected by keeping the concentrations of GDP-D-Glc low enough for not entering in competition with GDP-D-Man. As described in this study, GDP-D-Glc concentrations are indeed very low in wild-type worm and mouse tissues, which, in addition to the apparent absence of any physiological function of GDP-D-Glc in these species, supports the idea that GDP-D-Glc phosphorylase functions as a metabolite repair enzyme.

The concept of metabolite repair is based on the observation that certain enzymes are not as specific as generally stated and sometimes form "unwanted" side products by acting on cellular compounds different from their main substrate (39). A metabolite repair enzyme functions to specifically remove such unwanted side products. L-2-Hydroxyglutarate dehydrogenase is the first example of a metabolite repair enzyme that has been molecularly identified; it acts to remove the toxic product formed by L-malate dehydrogenase when this enzyme acts on α-ketoglutarate instead of its main substrate oxaloacetate (40). The physiological importance of this enzyme is demonstrated by the severe consequences of its deficiency, which leads to a neurometabolic disease known as L-2-hydroxyglutaric aciduria (39). GDP-D-Glc phosphorylase could serve to compensate for the lack of specificity of GDP-D-Man pyrophosphorylase, which, as described above, is quite active in forming GDP-D-Glc *in vitro* (10). It seems surprising that such an activity would

have been conserved if there is no need for GDP-D-Glc in the cell. It is therefore tempting to speculate that this enzyme is regulated intracellularly in a way that this GDP-D-Glc-forming activity of GDP-D-Man pyrophosphorylase is inhibited to a certain extent, potentially via its composition in α- and β-subunits. The remaining D-Glc-1-P guanylyltransferase activity could then be indirectly corrected by GDP-D-Glc phosphorylase through removal of the GDP-D-Glc formed (see Fig. 5). It can be noted here that the activity levels reported for D-Glc-1-P guanylyltransferase in mammalian tissues (8) are in the same range as the activity levels found in this study for GDP-D-Glc phosphorylase in mammalian tissues; in liver for example, a value of about 0.6 nmol min^{-1} mg of $protein^{-1}$ has been found for both of these activities. Combined with the high affinity for GDP-D-Glc that we determined for GDP-D-Glc phosphorylase, this enzyme has the required properties to efficiently remove the apparently useless GDP-hexose.

In this metabolite repair hypothesis, a deficiency in GDP-D-Glc phosphorylase activity could lead to GDP-D-Glc accumulation as we observed in worms deficient in this enzyme and subsequent erroneous incorporation of glucosyl units instead of mannosyl units into oligosaccharide chains (Fig. 5). If GDP-D-Glc is formed *in vivo* by GDP-D-Man pyrophosphorylase, the cytosolic mannosyltransferases (including ALG1, ALG2, and ALG11) involved in the protein *N*-glycosylation pathway should be most prone to encounter accumulating GDP-D-Glc molecules. These cytosolic mannosyltransferases successively add five mannosyl residues from GDP-D-Man to dolichol-PP-$(GlcNAc)_2$. The dolichol-PP-$(GlcNAc)_2Man_5$ intermediate is then flipped to the endoplasmic reticulum lumen where this lipid-linked oligosaccharide (LLO) is further extended and finally transferred to Asn residues on newly synthesized polypeptide chains (35). It is difficult to predict the consequences of the replacement of mannosyl residues by glucosyl residues in LLO, but, as for the numerous inherited deficiencies in LLO assembly (congenital disorders of glycosylation type I (CDG-I)) already identified, this could lead to the production of structurally incomplete LLOs, resulting in hypoglycosylation of multiple glycoproteins (35, 41). It will therefore be of great interest to screen for mutations in the *C15orf58* gene in CDG-I patients for which the basic defect has yet to be elucidated (CDG-Ix patients; Ref. 42). The high expression of GDP-D-Glc phosphorylase in the nervous system suggests a greater vulnerability of this organ to GDP-D-Glc accumulation, which is compatible with the pronounced neurological symptoms that are very commonly observed in CDG-I patients. As LLO is synthesized in *C. elegans* by the common eukaryotic pathway (43), the *C10F3.4* mutant strain might provide a good model for the identification of potential glycosylation defects caused by GDP-D-Glc phosphorylase deficiency. It should be noted, however, that worms appear to be more resistant to such defects than humans as no overt phenotypes have been observed upon RNA interference against certain genes of the LLO synthesis pathway in worms grown in standard culture conditions (43).

In conclusion, we identified a novel enzyme, GDP-D-Glc phosphorylase, potentially involved in metabolite repair in nematodes and mammals (Fig. 5). Ongoing work is designed to better understand the molecular basis of the GDP-D-Glc-forming activity of GDP-D-Man pyrophosphorylase and to test whether GDP-D-Glc phosphorylase is needed for functional glycoprotein biosynthesis.

Acknowledgments—We are indebted to Dr. Colin Thacker of the Worm Core Facility (University of Utah) for generating the transgenic C10F3.4::GFP fusion C. elegans strain. We sincerely thank Dr. Shohei Mitani (Tokyo Women's Medical University, Tokyo, Japan) for providing the C10F3.4 mutant strain (tm2679) and Prof. Shinichi Kitamura (Osaka Prefecture University, Osaka, Japan) for kindly providing GDP-L-galactose. We also thank our UCLA colleagues Drs. Alison Frand and Lars Dreier for sharing expertise and equipment for microscopy, Dr. Jonathan Lowenson for help in preparing mouse extracts, and Dr. Jonathan Wanagat for advice on quantitative PCR data analysis. Finally, we thank Prof. Emile Van Schaftingen (de Duve Institute, Brussels, Belgium) for critical reading of the manuscript.

REFERENCES

1. Linster, C. L., Gomez, T. A., Christensen, K. C., Adler, L. N., Young, B. D., Brenner, C., and Clarke, S. G. (2007) *J. Biol. Chem.* **282,** 18879–18885
2. Laing, W. A., Wright, M. A., Cooney, J., and Bulley, S. M. (2007) *Proc. Natl. Acad. Sci. U.S.A.* **104,** 9534–9539
3. Dowdle, J., Ishikawa, T., Gatzek, S., Rolinski, S., and Smirnoff, N. (2007) *Plant J.* **52,** 673–689
4. Linster, C. L., and Clarke, S. G. (2008) *Trends Plant Sci.* **13,** 567–573
5. Bulley, S. M., Rassam, M., Hoser, D., Otto, W., Schünemann, N., Wright, M., MacRae, E., Gleave, A., and Laing, W. (2009) *J. Exp. Bot.* **60,** 765–778
6. Linster, C. L., and Van Schaftingen, E. (2007) *FEBS J.* **274,** 1–22
7. Carlson, D. M., and Hansen, R. G. (1962) *J. Biol. Chem.* **237,** 1260–1265
8. Verachtert, H., Rodriguez, P., Bass, S. T., and Hansen, R. G. (1966) *J. Biol. Chem.* **241,** 2007–2013
9. Szumilo, T., Drake, R. R., York, J. L., and Elbein, A. D. (1993) *J. Biol. Chem.* **268,** 17943–17950
10. Ning, B., and Elbein, A. D. (2000) *Eur. J. Biochem.* **267,** 6866–6874
11. Brenner, C. (2002) *Biochemistry* **41,** 9003–9014
12. Brenner, C. (2007) *Encyclopedia of Life Sciences*, John Wiley & Sons, Ltd., Chichester, UK, doi: 10.1002/9780470015902.00020545
13. Watanabe, K., Suzuki, K., and Kitamura, S. (2006) *Phytochemistry* **67,** 338–346
14. Sulston, J., and Hodgkin, J. (1988) in *The Nematode Caenorhabditis elegans* (Wood W. B., ed) pp. 587–606, Cold Spring Harbor Laboratory Press, Cold Spring Harbor, NY
15. Lewis, J. A., and Fleming, J. T. (1995) *Methods Cell Biol.* **48,** 3–29
16. Brenner, S. (1974) *Genetics* **77,** 71–94
17. Kagan, R. M., and Clarke, S. (1995) *Biochemistry* **34,** 10794–10806
18. Hobert, O. (2002) *BioTechniques* **32,** 728–730
19. Webb, K. J., Lipson, R. S., Al-Hadid, Q., Whitelegge, J. P., and Clarke, S. G. (2010) *Biochemistry* **49,** 5225–5235
20. Nihira, T., Nakajima, M., Inoue, K., Nishimoto, M., and Kitaoka, M. (2007) *Anal. Biochem.* **371,** 259–261
21. Coulier, L., Bas, R., Jespersen, S., Verheij, E., van der Werf, M. J., and Hankemeier, T. (2006) *Anal. Chem.* **78,** 6573–6582
22. Chatterjee, I. B. (1973) *Science* **182,** 1271–1272
23. Massie, H. R., Shumway, M. E., Whitney, S. J., Sternick, S. M., and Aiello, V. R. (1991) *Exp. Gerontol.* **26,** 487–494
24. Linster, C. L., Adler, L. N., Webb, K., Christensen, K. C., Brenner, C., and Clarke, S. G. (2008) *J. Biol. Chem.* **283,** 18483–18492
25. Barber, G. A. (1985) *FEBS Lett.* **183,** 129–132
26. Spiro, M. J. (1984) *Diabetologia* **26,** 70–75

27. Mori, S., Shibayama, K., Wachino, J., and Arakawa, Y. (2010) *Protein Expr. Purif.* **69,** 99–105
28. Guranowski, A., Wojdyła, A. M., Zimny, J., Wypijewska, A., Kowalska, J., Jemielity, J., Davis, R. E., and Bieganowski, P. (2010) *FEBS Lett.* **584,** 93–98
29. Elbein, A. D. (1969) *J. Biol. Chem.* **244,** 1608–1616
30. Smith, M. M., Axelos, M., and Péaud-Lenoël, C. (1976) *Biochimie* **58,** 1195–1211
31. Piro, G., Zuppa, A., Dalessandro, G., and Northcote, D. H. (1993) *Planta* **190,** 206–220
32. Liepman, A. H., Wilkerson, C. G., and Keegstra, K. (2005) *Proc. Natl. Acad. Sci. U.S.A.* **102,** 2221–2226
33. Elbein, A. D., Pan, Y. T., Pastuszak, I., and Carroll, D. (2003) *Glycobiology* **13,** 17R–27R
34. Smoot, J. W., and Serif, G. S. (1985) *Eur. J. Biochem.* **148,** 83–87
35. Varki, A., Cummings, R. D., Esko, J. D., Freeze, H. H., Stanley, P., Bertozzi, C. R., Hart, G. W., and Etzler, M. E. (eds) (2009) *Essentials of Glycobiology*, 2nd Ed., pp. 50–56, 104–112, 586–592, Cold Spring Harbor Laboratory Press, Cold Spring Harbor, NY
36. Roberts, I. S. (1996) *Annu. Rev. Microbiol.* **50,** 285–315
37. Behrens, N. H., and Cabib, E. (1968) *J. Biol. Chem.* **243,** 502–509
38. Zea, C. J., and Pohl, N. L. (2005) *Biopolymers* **79,** 106–113
39. Van Schaftingen, E., Rzem, R., and Veiga-da-Cunha, M. (2009) *J. Inherit. Metab. Dis.* **32,** 135–142
40. Rzem, R., Vincent, M. F., Van Schaftingen, E., and Veiga-da-Cunha, M. (2007) *J. Inherit. Metab. Dis.* **30,** 681–689
41. Haeuptle, M. A., and Hennet, T. (2009) *Hum. Mutat.* **30,** 1628–1641
42. Jaeken, J. (2010) *Ann. N.Y. Acad. Sci.* **1214,** 190–198
43. Struwe, W. B., and Warren, C. E. (2010) *Methods Enzymol.* **480,** 477–493